



Structural Behaviour of Clay Brick Lime Mortar Masonry Walls Under Lateral Cyclic Loading in Dry and Wet Conditions

A. Y. Elghazouli¹(✉), D. V. Bompa^{1,2}, S. A. Mourad³, and A. Elyamani⁴

¹ Department of Civil and Environmental Engineering, Imperial College London, London, UK
a.elghazouli@imperial.ac.uk

² Department of Civil and Environmental Engineering, University of Surrey, Guildford, UK

³ Department of Structural Engineering, Cairo University, Giza, Egypt

⁴ Department of Archeological Conservation, Cairo University, Giza, Egypt

Abstract. This paper examines the experimental structural response of clay brick lime mortar masonry walls in wet and ambient-dry conditions. The properties of fired-clay bricks and hydraulic lime-mortar materials are selected to resemble those of existing heritage masonry structures in Historic Cairo. The investigation includes tests on square panels under diagonal compression, and large-scale walls subjected to gravity loading and in-plane lateral cyclic displacements. In addition to the conditioning type, the effectiveness of strengthening with helical bars in horizontal bed joints is also investigated. Implications of embedding helical bars in lime mortar as well as the provision of end anchorages are assessed. The complete load-deformation response of the large-scale members is also evaluated, including the main behavioural characteristics and failure modes. The results show that moisture has a notable effect on the main mechanical properties and overall structural response of such masonry components. For the panels subjected to diagonal compression, the strength reduction under wet conditions is shown to be more than 40% compared to the dry counterparts. For the large-scale walls, subjected to combined lateral loading and precompression, this reduction is significantly lower but can exceed 10%. It is also shown that the provision of helical bars can, depending on their end anchorage and arrangement, double the diagonal tension strength of masonry and offset the adverse effects occurring due to moisture.

Keywords: Masonry walls · Lime mortar · Clay bricks · Wet conditions · Diagonal tension · Lateral deformation · Cyclic loading

1 Introduction

Heritage masonry is characterised by high material heterogeneity, irregular bearing elements and degradation of constituents due to environmental effects. It is recognised that environmental wet-dry cycling can affect both the mechanical characteristics of masonry as well as plaster and rendering (Cotic et al. 2013; Gentilini et al. 2015). Unreinforced masonry walls can develop shear- or flexure-governed failures depending on

their geometry, aspect ratio and boundary conditions. The diagonal shear and sliding strength of URM is greatly dependent on the mortar-brick interaction. In general, the interface mortar-brick shear response greatly depends on the moisture content, porosity, mortar strength, and conditioning type (Mazzotti et al. 2014; Bompa and Elghazouli 2020a), with saturation causing a deterioration in strength and stiffness (Franzoni et al. 2015; Bompa and Elghazouli 2020b).

The ductility and robustness of lateral-resisting masonry elements are of particular importance for structures subjected to seismic loading (Elghazouli 2016). To this end, previous studies have shown that the geometry, coupling level, and material properties, influence not only the strength but also the deformation capacity and cyclic degradation of masonry (Vasconcelos and Lourenço 2009). Comparative cyclic tests on dry low-strength mortar masonry also indicated a modification in failure mode from combined rocking-shear to rocking when the height-to-depth aspect ratio increased from 0.7 to 1.4, representative of squat and slender elements, respectively (ElGawady et al. 2005). Other tests on small-scale dry historic masonry exhibited diagonal-cracking failures, reaching ultimate drifts below 0.4% (Capozucca 2011).

Although experimental assessments on ambient-dry masonry walls representative of heritage structures have been carried out (Calvi et al. 1996), studies to investigate the lateral cyclic performance of wet large-scale masonry are lacking, and the influence of moisture on the diagonal cracking response has also not been examined. Such masonry structures are typically also not specifically designed for resisting lateral seismic loading.

This paper therefore presents an experimental investigation into the material and structural response of ambient-dry and wet masonry elements consisting of fired clay brick and hydraulic lime mortar, which are used in many historic structures. The properties of the fired-clay bricks and lime-mortar materials were selected to resemble those of masonry components investigated in a wider research programme on the management and conservation of heritage masonry structures in Historic Cairo.

2 Experimental Programme

2.1 Material Properties

Commercial fired clay facing solid bricks with measured sizes of $229 \times 110 \times 66$ mm were used for the construction of all specimens. The measured average compressive strength of brick units parallel to the testing bed, obtained from a minimum of three tests, was about 15.5 MPa in both dry and wet conditions, with the latter corresponding to full submersion in water for 48 h. From readily available materials, this type of fired-clay bricks has the closest physical and mechanical properties to those from the Mausoleum of Fatima Khatun (Umm al-Salih) built in the 13th century in Cairo, which is assessed in the project. Site surveys indicated that: (i) 'red' bricks (used for the foundation) have a compressive strength (f_b) of about 5.2 MPa and water absorption $w_a = 27.5\%$, (ii) 'light brown' bricks have an $f_b = 14.7$ MPa and $w_a = 18.13\%$ and (iii) 'dark brown' bricks have an $f_b = 22.7$ MPa and $w_a = 13.4\%$.

The characteristics of the selected fired-clay bricks are hence within the range of those from the site survey, typically found in such heritage masonry, and can be used for comparative assessments and structural repair studies. The moisture content of both

conditioning cases for bricks was assessed. The ambient-dry samples and those submersed in tap water for a minimum of 48 h, were dried in an oven for 6 h at 60 °C and another for 18 h at 105 °C until the sample mass was relatively constant. The moisture content of ambient-dry bricks was 0.07% by weight (wt.%), and 10.46 wt.% for those submersed in water.

Mortars incorporating natural hydraulic lime (NHL5) with a binder-to-aggregate ratio of 1:3 were selected for the study as these are typically used for conservation works. These are singular binders which combine hydraulic with air setting, obtained by carbonation with atmospheric CO₂. The free lime Ca(OH)₂ is above 15%, whilst the sulphates content is below 2%.

Compressive strengths on a minimum of 5 samples for each masonry specimen were determined from compression tests on ambient-dry and wet cubes (50 × 50 × 50 mm). The resulting strengths of the mortars in ambient-dry conditions were between $f_{lm} = 2.08 - 5.11$ MPa, and in wet conditions were between $f_{lm} = 0.70 - 2.37$ MPa (Table 1 and 2). An average reduction in elastic modulus in the range of 50% was also typically observed due to moisture. Additionally, the moisture content of both conditioning cases for NHL mortar samples was assessed following the same procedure as for the bricks. The moisture content of the lime mortars was 2.54% by weight (wt.%) for ambient-dry samples and 10.80 (wt.%) for those submersed in water.

2.2 Diagonal Panels

Diagonal panel tests on single leaf square panels of $b \times h \times t = 710 \times 710 \times 110$ mm in wet and air-dry conditions were carried out in order to assess the diagonal tensile strength of masonry (Fig. 1). These were either non-strengthened or strengthened with helical bars. The specimen reference adopts the following formats: DB-Xx for non-strengthened specimens, and DHx-Yy for strengthened specimens. For non-strengthened members (DB-Xy), X refers to conditioning D-dry or W-wet, and y to testing sequence, whilst for the strengthened specimens (DHx-Yy), x stands for end anchorage (N – not present, A – end anchorage), Y refers to conditioning as above, and y is for the testing sequence.

The panels for diagonal testing, as depicted in Fig. 1a, b, had both horizontal and vertical lime mortar joints with an average thickness of 9 ± 1.5 mm. After the last course of bricks was laid, the specimens were kept in laboratory conditions. Plastic sheets were used to cover the specimens at early curing, and they were then tested at an age of 30–35 days. Helical stainless-steel reinforcing bars for masonry repair were used in four diagonal panels and two large-scale tests.

Four bars of 4.5 mm and proof stress around 1100 N/mm² were used per specimen. These were directly incorporated in the third and the sixth bed joints of the panels as shown in yellow in Fig. 1b. Two bars were embedded in the lime mortar laid in each of the two horizontal joints, at 30 mm from the face of the panel. The helical bars from Specimens DHA were provided with end anchorage systems to prevent slip, whilst Specimens DHN had only straight bars.

Prior to testing, the wet specimens were submersed 3/5 of depth in water and were sprinkled with a hose from the top. After testing, the walls were dismantled, and samples were extracted to assess the moisture content. After each brick and mortar joints were weighed, all components were dried in an oven for 6h at 60 °C for at least 18h at 105 °C

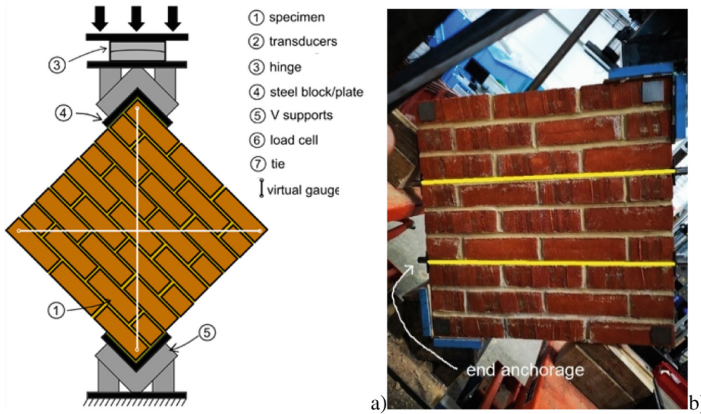


Fig. 1. (a) Arrangement of diagonal tests, (b) Strengthening details

until reaching a constant mass. The moisture distribution results indicated that the same moisture content of $10.7\% \pm 0.2$ wt was consistently obtained in all nine brick courses. Cylinders of diameter $d = 69$ mm and height of around $h = 145$ mm were extracted, after testing, from undamaged areas of the diagonal panels to assess the compression properties of the masonry. The compressive strengths of masonry (f_m) from cylinder testing are given in Tables 1 and 2.

The tests on diagonal panels were carried out in a rig which included a main loading transfer frame with a 1000 kN Instron actuator and a connected load cell. As shown in Fig. 1a, the specimens were positioned and loaded through V-shaped supports. External transducers were used for secondary measurements alongside the displacement recordings provided by the machine, coupled with detailed data from a Digital Image Correlation (DIC) system (Elghazouli et al. 2021).

2.3 Large Walls Under Combined Loading

Single leaf masonry walls of 1910 mm length, 1300 mm height and 110 mm width were built using fired-clay bricks and lime mortars, as described above. A total of four selected tests on walls under combined loading are presented in this section. All specimens were tested under lateral cyclic loading and a representative gravity load of about 1.0 MPa.

The specimen reference adopts the format WX-Y, where W stands for wall, X represents the specimen type: (B for non-strengthened specimens or H for members with helical bars), and Y represents the conditioning (D for air-dry or W for wet). For example, WB-D is a non-strengthened ambient-dry wall. From the two non-strengthened walls, one was tested in wet conditions and the other in dry conditions. The same approach was applied to the two strengthened walls.

Stretcher/running bond was used to construct the 16 course high walls (Fig. 2). To achieve the desired specimen height, the mortar joint thickness was in the range of 8–10 mm. For the strengthened walls, a total of four bars were inserted in two bed joints located above the fifth and eleventh brick course from the bottom to the top of the wall. The helical bars were positioned directly in the lime mortar layer. All bars were provided

with end anchorages as a secondary force transfer mechanism along with the bar-mortar bond. The properties of the helical bars used in the large walls were identical to those used for the diagonal panels described above.

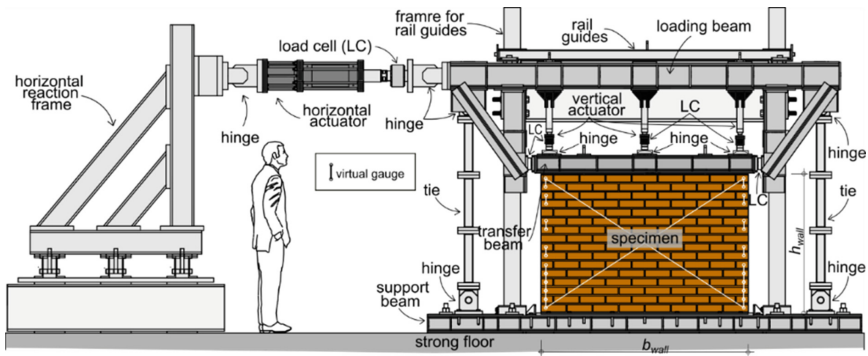


Fig. 2. Testing arrangement for large scale walls

To enable wetting through capillary absorption of wet walls, after the specimens were placed in the testing rig and the prestressing ties were removed, a water tank was built in-place which was connected to the first course of bricks. In addition to the water tank, a pipe/sprinkler system mounted at the top of the wall was manufactured and was used to accelerate the wetting process. The conditioning procedure was identical for both non-strengthened walls and those with helical bars. The moisture content of samples from the tested walls was assessed similarly to the diagonal panels. The average moisture content was 11.1% by weight with a standard deviation was 0.34%, indicating that the moisture was evenly spread.

The rig shown schematically in Fig. 2 was designed to enable realistic experimental assessment of the ultimate behaviour of large-scale members subjected to lateral cyclic displacements and co-existing axial loading. The specimens were directly supported by a 25 mm thick plate and connected by means of prestressed $\text{Ø}20$ mm bolts to a supporting steel beam. The latter was connected to the strong floor by means of $4 \times \text{Ø}33$ mm prestressing ties to avoid sliding and overturning under lateral loads. At the top of the wall, three 120 kN Enerpac actuators were connected to a steel loading beam and were used to apply the gravity load by means of unidirectional hinges to the specimen through a transfer steel beam.

For the application of the lateral loading, another 250 kN Instron actuator was placed horizontally and connected to the reaction frame. After the application of the constant vertical load, corresponding to an axial stress around 1.0 MPa, the lateral deformations were applied based on a pre-defined quasi-static cyclic history. A set of three cycles were applied for each deformation level, corresponding to a drift of 0.025, 0.050, 0.075, 0.10, 0.15, 0.20, 0.25, 0.30, 0.35, 0.40, 0.50, 0.80, 1.0, 1.25, 1.50 (%). The displacement rate and loading procedure were chosen based on recommendations available in the literature (Petry and Beyer 2015; Magenes et al. 2008).

3 Test Results and Observations

3.1 Diagonal Panels

Table 1 depicts the main results of the tested panels, whilst Fig. 3 illustrates a typical crack pattern and failure characteristics for selected members. In the diagonal panel tests, when the principal tensile stresses perpendicular to the compressed strut reached the maximum tensile strength, failure occurred due to bond failure between the brick unit and the mortar in the joints. In terms of the crack kinematics, similar behaviour was observed during tests on both air-dry and wet specimens. Close inspection of the results showed that the moisture reduced both the stiffness and the specimen strength, albeit with different extents as a function of mortar strengths (Elghazouli et al. 2021).

Table 1. Main results of diagonal panel tests

Specimen	P(kN)	$\alpha(^{\circ})$	f_m (MPa)	f_{lm} (MPa)	Specimen	P(kN)	$\alpha(^{\circ})$	f_m (MPa)	f_{lm} (MPa)
DB-D1	48.0	39.7	5.70	2.53	DHN-D1	66.2	31.3	5.70	2.13
DB-D2	53.1	38.4	5.70	2.25	DHN-D2	63.4	35.6	5.70	2.09
DB-D3	52.3	40.3	6.06	2.56	DHA-D1	128.3	42.7	6.06	2.09
DB-W1	26.5	39.3	4.28	0.70	DHA-W1	62.9	34.6	4.78	0.98
DB-W2	31.5	39.8	4.28	0.70					

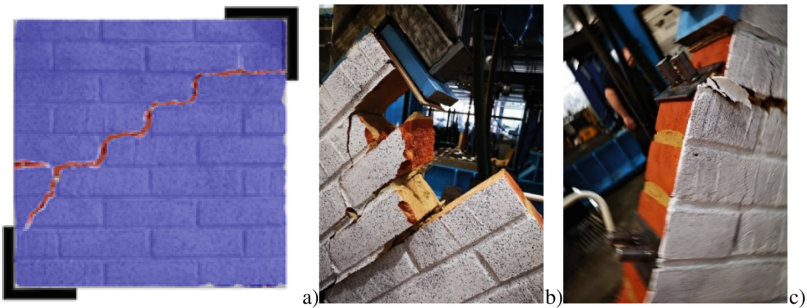


Fig. 3. (a) typical crack pattern, (b) failure characteristics of DHN Specimens, (c) failure characteristics of DHA Specimens

The response of dry panels was generally characterised by loss of bond at a horizontal bed joint at the centre of the panel at around 80–90% of the peak capacity P_u . The critical crack propagated following the top and bottom plates through vertical and horizontal bed joints in a stepped mode. As shown in Fig. 4a, failure largely occurred due to a single diagonal crack. For wet panels, the failure patterns resembled those of their corresponding dry counterparts. However, the first strain concentrations associated with loss of bond at the brick-to-mortar interface occurred at 73–75% of P_u .

Dry specimens provided with helical bars and no end anchorage (DHN-D) showed a modest strength increase of about 12–17% compared to their non-strengthened counterparts, as indicated in Table 1. The strength increase was modest because the critical crack passed only through one of the reinforced bed joints, and the bond between the lime mortar and helical bars was relatively low. In contrast, when the bars were provided with end anchorages the strength increase was by a factor of 2.28 (DHA-D) compared to the non-strengthened dry specimens. When helical bars were used with anchorage and in wet conditions, the contribution of the strengthening system was largely offset by the presence of moisture (Specimen DHA-W1).

3.2 Large Scale Walls

The complete load-drift ($P-\Delta$) curves of the tested walls are shown in Fig. 4. The crack patterns at failure obtained from DIC recordings are illustrated in Fig. 5, and the main test results are given in Table 2. The $P-\Delta$ response of the air-dry Specimen WB-D and its envelope are illustrated in Fig. 4a, and the failure patterns are shown in Fig. 5a. The lateral deformation at peak corresponded to a drift of $\Delta_{\text{peak}+} = 0.53\%$ and $\Delta_{\text{peak}-} = 0.53\%$ in the push (positive) and pull (negative) cycle (Table 2). The corresponding maximum lateral load carrying capacity was $P_{u+} = 146.3$ kN and $P_{u-} = 142.2$ kN, respectively. The transition between elastic and inelastic stiffness occurred at a lateral load (P) around 80 kN in both loading directions. This corresponded to a drift ratio of about $\Delta = 0.1\%$ and was associated with initial signs of cracking. At this stage, the behaviour was largely governed by flexure.

The first visible diagonal crack occurred in the negative (pull) cycle at a drift level $\Delta = 0.53\%$ and closed during unloading. At the same drift level in the push (positive cycle), a diagonal crack nearly perpendicular to that occurring from the pull cycle was initiated. This corresponded to the maximum capacity of the specimen. At the third displacement cycle in the positive direction, the specimen failed and was unable to reach the load attained in the previous cycles. The ultimate drifts, assumed to correspond to 20% reduction in load carrying capacity (Bompa and Elghazouli 2019), were $\Delta_{u+} = 0.61\%$ and $\Delta_{u-} = 0.58\%$.

Specimen WB-W was tested in wet conditions. The full load-drift ($P-\Delta$) and envelope curves are depicted in Fig. 4b, while the crack patterns at failure are shown in Fig. 5b. A noticeable reduction in stiffness started at about 35kN ($\Delta = 0.07\%$) then at 95 kN ($\Delta = 0.25\%$). The initial stiffness was $K_0 = 75.6$ kN/mm. The maximum lateral load was $P_{u+} = 127.0$ kN and $P_{u-} = 129.2$ kN in the two directions, corresponding to drifts of $\Delta_{\text{peak}+} = 0.35\%$ and $\Delta_{\text{peak}-} = 0.31\%$ in the push (positive) and pull (negative) cycles, respectively. The behaviour of WB-W was initially governed by flexure. The first signs of diagonal cracking were observed at around $\Delta = 0.20\%$, with the maximum capacity reached closely after. Failure was characterised by sliding along the diagonal cracks.

Specimen WH-D had helical bars and was tested under combined axial load and lateral cyclic displacement, in dry condition. The complete load-drift ($P-\Delta$) and crack patterns at failure are illustrated in Fig. 4c and Fig. 5c. The maximum lateral load carrying capacity was $P_{\text{max, pos}} = 134.1$ kN and $P_{\text{max, neg}} = -142.2$ kN, respectively. This corresponded to a drift of $\Delta_+ = 0.55\%$ and $\Delta_- = -0.55\%$ in the push (positive) and pull (negative) cycle. The first inclined crack occurred in the second pull (negative) cycle

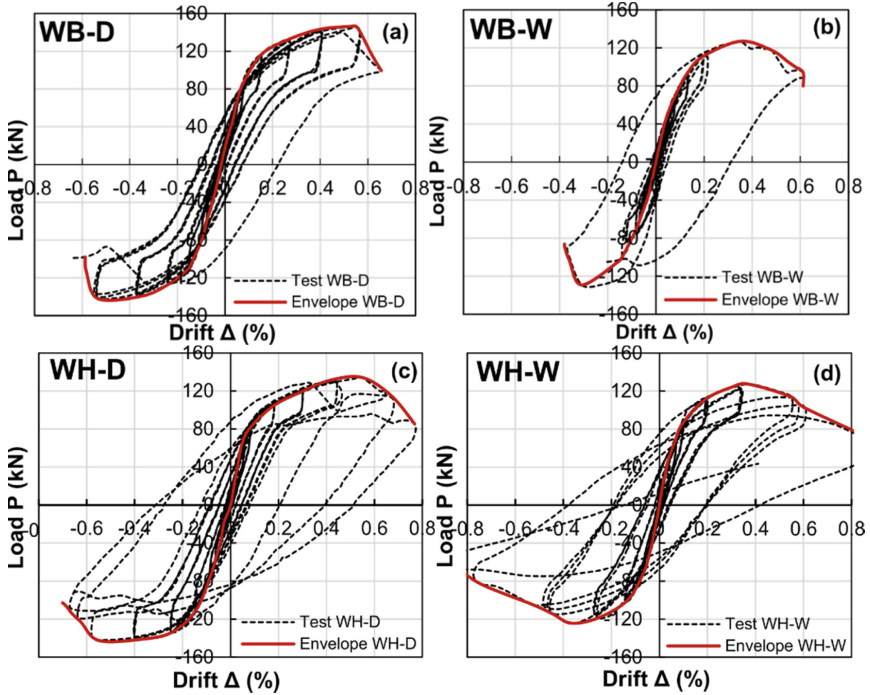


Fig. 4. Load-drift ($P-\Delta$) curves of (a) WB-D, (b) WB-W, (c) WH-D, (d) WH-W

Table 2. Main test results from tests on large scale walls

	P_{u+} (kN)	P_{u-} (kN)	P_u (kN)	Δ_{peak+} (%)	Δ_{peak-} (%)	Δ_{u+} (%)	Δ_{u-} (%)	K_{test} (kN/mm)	f_m (MPa)	f_{lm} (MPa)
WB-D	146.3	142.2	144.3	0.53	0.53	0.61	0.58	68.4	6.59	5.11
WB-W	127.0	129.2	128.1	0.35	0.31	0.57	0.36	54.6	6.04	2.36
WH-D	134.1	142.2	138.2	0.55	0.55	0.70	0.67	89.6	6.06	3.12
WH-W	127.6	124.5	126.1	0.37	0.37	0.61	0.58	96.0	4.87	1.62

at drift around a drift of 0.20%. As the helical bars kept the crack closed at displacement reversal, weaker regions developed outside of the shear-reinforced regions. Hence, a sliding crack occurred below the third brick course from top to bottom. This was followed by an inclined crack in the push (positive) cycle. Ultimately, failure was due to the sliding of the top non-reinforced region. The ultimate drifts were $\Delta_{u+} = 0.70$ and $\Delta_{u-} = 0.67$, in the positive and negative loading direction, respectively.

Specimen WH-W had helical bars and was tested in wet condition. The complete load-drift ($P-\Delta$) and crack patterns at failure are illustrated in Fig. 4d and 5d, respectively. The maximum lateral load carrying capacity was $P_{max,pos} = 127.6$ kN and $P_{max,neg} = -124.5$ kN, respectively. This corresponded to drifts of $\Delta_+ = 0.37\%$ and $\Delta_- = -0.37\%$ in the positive and negative cycles. The first inclined crack occurred in the third negative cycle at a drift of 0.38%. For the wet wall, the presence of the helical bars seems to have

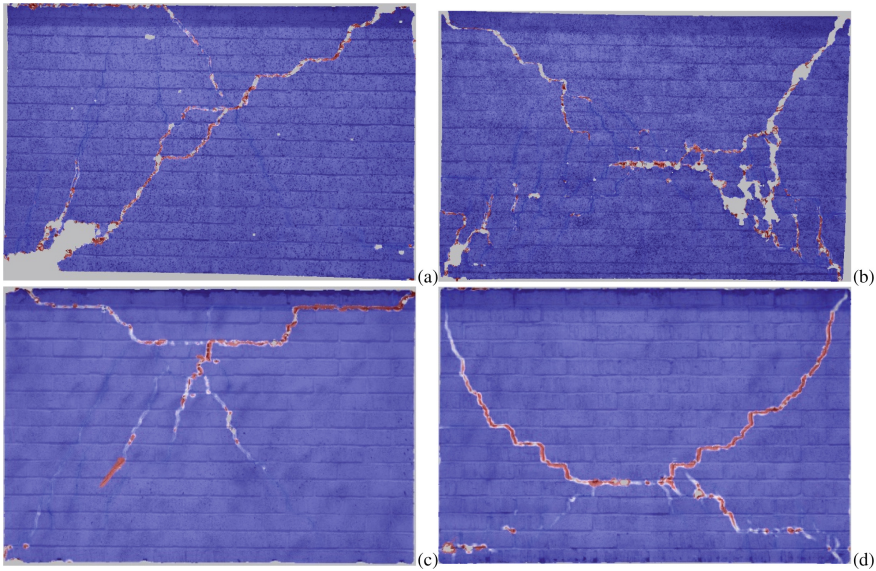


Fig. 5. Crack patterns at failure for Specimens: (a) WB-D, (b) WB-W, (c) WH-D, (d) WH-W

created a weak region at the bottom bed joint. The horizontal crack where the two inclined cracks intersect correspond to the position of the helical bars.

Comparing the response of the wet (WB-W and WH-W) and dry (WB-D and WH-D) specimens, the influence of moisture on the capacity of the members becomes evident. For the wet walls, the average reduction in lateral strength was about 11%, whilst the reduction in stiffness was around 20% compared to the dry walls. These ranges are significantly lower both in terms of stiffness and strength than the differences between wet and dry properties obtained from the diagonal panel tests. This is attributed to the different loading and failure conditions with respect to mortar and brick interaction.

Specimens WB-D and WB-W had a flexure-governed response characterised by opening of an interface gap between the supporting plate and the first brick course. The response of both WH-D and WH-W walls was largely symmetric and governed by shear, ultimately failing in diagonal tension with the two diagonal cracks intersecting outside of the region reinforced with helical bars. Unreinforced masonry can develop such response, as often explained by aspects of non-linear elastic behaviour (Petry and Beyer 2015). This is mainly attributed to the reduction of the compression zone with the increase in lateral displacement and the associated decrease in effective stiffness of the member. The contribution of the tension side of the wall also gradually diminishes as cracks open along the horizontal bed joints.

As discussed above, the ductility of the wet walls, in terms of ultimate drift, was broadly similar or lower than that of their dry counterparts, primarily influenced by the post-peak kinematics. Given the influence of moisture on the stiffness and effective yield, perhaps a more representative measure of ductility would be an ultimate-to-yield drift ratio ($\mu_{\Delta} = \Delta_u/\Delta_y$). The yield drift can be estimated from a simplified bilinear P- Δ curve by equating areas under the average test P- Δ envelope and the bilinear P- Δ

idealisation. Using this approach, the drift ductility ratios (μ_{Δ}) are estimated as 4.0 for WB-D, 3.5 for WB-W, 4.8 for WH-D and 4.2 for WH-W. Overall, direct experimental comparison between the cyclic response of the wet and dry specimens shows the negative effect of moisture on the stiffness, capacity and ductility of masonry walls subjected to initial gravity and increasing lateral loads.

4 Concluding Remarks

This paper presented an experimental investigation into the response of ambient-dry and wet clay-brick/lime-mortar masonry elements representative of those in some historic structures. Several tests on large-scale walls subjected to gravity load and lateral displacements as well as square panels under diagonal compression, were described. Although, as expected, there is significant inherent variability in the properties of masonry elements, depending on the constituent materials and construction conditions, this investigation offered an insight into the influence of moisture on the behaviour.

A direct comparison between strength properties of dry and wet specimens tested under diagonal compression showed that moisture reduced the strength on average by about 47% of the dry specimens, respectively. Full-field DIC measurements also showed that the cracking load was reduced by moisture with the brick-to-mortar interface bond loss occurring at around 75% and 85% of ultimate for the wet and dry specimens, respectively. Specimens provided with helical bars and no end anchorage showed a modest strength increase compared to their non-strengthened counterparts. In contrast, when the bars were provided with end anchorages, the strength increase was by a factor of 2.28. For the cylindrical cores tested in this study, the reduction in the elastic modulus and compressive strength was on average in the range of 13% and 15%, respectively, between the dry and wet cases.

Large-scale tests on masonry walls under cyclic loading and practical levels of gravity load indicated up to 11% reduction in lateral strength in the presence of moisture. Although these ranges are significantly lower than those obtained from the diagonal panel tests, due to the different loading and failure conditions, the combined results show that notable reductions in elastic and ultimate properties would occur when the masonry is wet. All non-strengthened specimens tested under cyclic loading had a brittle failure in diagonal tension. For the dry strengthened wall, the helical bars kept the crack closed at displacement reversal, and weaker regions developed outside of the reinforced regions. For the wet wall, the presence of the helical bars created a weak region at the bottom bed joint, similarly shifting the critical cracks outside the reinforced region. The results and failure mode point to the need for further examination of various effective arrangements and extent of the helical bars in such large elements. Overall, the ultimate deformations of the wet cyclic walls were either broadly similar or lower than that of the dry counterparts. The wet walls also had ductility ratios about 10% lower than their dry counterparts.

Acknowledgements. The study was supported by the Arts and Humanities Research Council of the UK Research and Innovation agency, within the project “Interdisciplinary approach for the management and conservation of UNESCO World Heritage Site of Historic Cairo - Application

to Al-Ashraf Street”, Grant No. AH/R00787X/1. The authors would like to acknowledge the support provided by the technical staff of the Structures Laboratories at Imperial College London, particularly Mr. P. Crudge, Mr. L. Clark, and Mr. T. Stickland.

References

- Bompa, D.V., Elghazouli, A.Y.: Inelastic cyclic behaviour of RC members incorporating threaded reinforcement couplers. *Eng. Struct.* **180**, 468–483 (2019). <https://doi.org/10.1016/j.engstruct.2018.11.053>
- Bompa, D.V., Elghazouli, A.Y.: Experimental and numerical assessment of the shear behaviour of lime mortar clay brick masonry triplets. *Constr. Build. Mater.* **262**, 120571 (2020a). <https://doi.org/10.1016/j.conbuildmat.2020.120571>
- Bompa, D.V., Elghazouli, A.Y.: Compressive behaviour of fired-clay brick and lime mortar masonry components in dry and wet conditions. *Mater. Struct.* **53**, 60 (2020b). <https://doi.org/10.1617/s11527-020-01493-w>
- Calvi, G.M., Kingsley, G.R., Magenes, G.: Testing of masonry structures for seismic assessment. *Earthq. Spectra* **12**(1), 145–162 (1996). <https://doi.org/10.1193/1.1585872>
- Capozucca, R.: Experimental analysis of historic masonry walls reinforced by CFRP under in-plane cyclic loading. *Compos. Struct.* **94**(1), 277–289 (2011). <https://doi.org/10.1016/j.compstruct.2011.06.007>
- Cotic, P., et al.: Effect of moisture on the reliability of void detection in brickwork masonry using radar, ultrasonic and complex resistivity tomography. *Mater. Struct.* **46**(10), 1723–1735 (2013). <https://doi.org/10.1617/s11527-012-0011-3>
- ElGawady, M.A., Lestuzzi, P., Badoux, M.: In-plane seismic response of URM walls upgraded with FRP. *J. Compos. Constr.* **9**(6), 524–535 (2005). [https://doi.org/10.1061/\(ASCE\)1090-0268\(2005\)9:6\(524\)](https://doi.org/10.1061/(ASCE)1090-0268(2005)9:6(524))
- Elghazouli, A. (ed.): *Seismic Design of Buildings to Eurocode 8*. CRC Press, Boca Raton (2016)
- Elghazouli, A.Y., Bompa, D.V., Mourad, S.A., Elyamani, A.: In-plane lateral cyclic behaviour of lime-mortar and clay-brick masonry walls in dry and wet conditions. *Bull. Earthq. Eng.* **19**, 5525–5563 (2021). <https://doi.org/10.1007/s10518-021-01170-5>
- Franzoni, E., Gentilini, C., Graziani, G., Bandini, S.: Compressive behaviour of brick masonry triplets in wet and dry conditions. *Constr. Build. Mater.* **82**, 45–52 (2015). <https://doi.org/10.1016/j.conbuildmat.2015.02.052>
- Gentilini, C., Franzoni, E., Graziani, G., Bandini, S.: Mechanical properties of fired-clay brick masonry models in moist and dry conditions. In: *Key Engineering Materials*, vol. 624, pp. 307–312. Trans Tech Publications Ltd. (2015). <https://doi.org/10.4028/www.scientific.net/KEM.624.307>
- Magenes, G., Morandi, P., Penna, A.: D 7.1 c Test results on the behaviour of masonry under static cyclic in plane lateral loads. Test report, ESECMaSE Project, University of Pavia, EURCENTRE, Italy (2008)
- Mazzotti, C., Sassoni, E., Pagliai, G.: Determination of shear strength of historic masonries by moderately destructive testing of masonry cores. *Constr. Build. Mater.* **54**, 421–431 (2014). <https://doi.org/10.1016/j.conbuildmat.2013.12.039>
- Petry, S., Beyer, K.: Force–displacement response of in-plane-loaded URM walls with a dominant flexural mode. *Earthq. Eng. Struct. Dynam.* **44**(14), 2551–2573 (2015). <https://doi.org/10.1002/eqe.2597>
- Vasconcelos, G., Lourenço, P.B.: In-plane experimental behavior of stone masonry walls under cyclic loading. *J. Struct. Eng.* **135**(10), 1269–1277 (2009). [https://doi.org/10.1061/\(ASCE\)ST.1943-541X.0000053](https://doi.org/10.1061/(ASCE)ST.1943-541X.0000053)